

AUTOMATIC ROAD VECTOR EXTRACTION FOR MOBILE MAPPING SYSTEMS

WANG Cheng^a, T. Hassan^b, N. El-Sheimy^b, M. Lavigne^b

^aSchool of Electronic Science and Engineering, National University of Defence Technology, China - chwang_nudt@263.net

^bDept of Geomatics Eng., 2500 University Drive, N.W, The tfabbas@ucalgary.ca of Calgary, Calgary, AB, Canada, T2N 1N4 - tfabbas@ucalgary.ca, naser@geomatics.ucalgary.ca, mlavigne@amsvisat.com

Commission III: WG III/5

KEY WORDS: Mobile Mapping, Computer Vision, Road Geometry, Lane Line, Automatic Extraction, VISAT™

ABSTRACT: Land-based mobile mapping systems have yielded an enormous time saving in capturing road networks and their surrounding. However, the manual extraction of the road information from the mobile mapping data is still a time-consuming task. This paper presents ARVEE (Automated Road Geometry Vectors Extraction Engine), a robust automatic road geometry extraction system developed by Absolute Mapping Solution Inc. (AMS). The extracted road information includes 3D continuous lane lines, road edges as well as lane lines attributes. There are three innovations in this work. First, all the visible lane lines in the georeferenced image sequences are extracted, instead of only extracting the central lane line or the nearby lane line pair. Second, lane line attributes are recognized, so the output is a functional description of the road geometry. Third, the output is an absolute-georeferenced model of lane lines in mapping coordinates, and is directly compatible to GIS databases. ARVEE includes four steps: First, extracting linear features in each image. Second, extracting, filtering and grouping linear features into lane line segments (LLS) based on their geometric and radiometric characteristics. Third, linking the LLSs into long lane lines 3D model using Multiple-Hypothesis Analysis (MHA). Finally, classifying each lane line into a lane line type based on the synthetic analysis of the included LLSs' features. The system has been tested on large number of VISAT™ mobile mapping data. The experiments on massive real MMS data sets demonstrate that ARVEE can deliver accurate and robust 3D continuous functional road geometry model. Full automatic processing result from ARVEE can replace most of the human efforts in road geometry modelling

1. INTRODUCTION

Mobile Mapping Systems (MMS), provide an effective way to collect georeferenced image sequences of the roads and their surroundings. For instance, the VISAT™ (Video-Inertial-Satellite) (El-Sheimy, 1999) developed by Absolute Mapping Solution Inc. (AMS) can be operated at road speed of up to 100 km/hr and achieve absolute positioning accuracy better than 0.3 m (RMS) for points within the field of view of the images captured by the van. Mobile mapping has yielded an enormous time saving in road network survey. However, the manual extraction of the road information from the mobile mapping data is still a time-consuming task.

Previous researches on lane line extraction mainly focus on the traffic applications, such as traffic monitoring or autonomous vehicle guidance (Ishikawa, 1988; Kenue, 1991; Jochem, 1993; Chen, 1997; Beauvais, 2000; Paetzold, 2000; Yim, 2003; Li, 2004; McCall, 2004; Tai, 2004; Yue Wang, 2004; Hassouna, 2005; Jung, 2005; Lee, 2005; Choi, 2006), more details can be found in (Kastrinaki, 2003). In summary, the constraints used in lane line detection include: (a) the shape, the lane lines is supposed to be a solid or dashed line with a certain width; (b) the colour, the lane lines are usually white or yellow; and (c) the geometry constrain, the road is flat and the lane lines are with almost no horizontal curvature. Led by the application purpose, and limited by the demand of real-time processing, these works only concerned about lane lines that are close to the vehicle, and all the results are described within local body frame coordinate, or even simply within the image coordinate frame. In addition, only vision sensors were exploited, and therefore, performances are generally not satisfying at the situation of obscuration, shadow or worn out painting. Few research works have focused on lane line extraction in image sequences using

georeferencing information from other sensing devices. For autonomous vehicle guidance, Radar and camera fusion were used to locate obstacle and lane line (Beauvais, 2000); location sensing devices, such as GPS, were fused with vision in lane lines following (Goldbeck, 2000; Jin Wang, 2005). In mobile mapping, Tao (Tao, 2001) used georeferenced images from mobile mapping image sequences to extract the 3D model of central lane line. Roncella (Roncella, 2006) developed a semi-automatic lane line extraction system and tested on synthetic mobile mapping data.

Recently, we developed ARVEE (Automated Road Geometry Vectors Extraction Engine) – a robust automatic road geometry extraction system for the post processing of georeferenced images captured by a land-based mobile mapping system. The input of the system is the mobile mapping data, which includes: georeferencing information, multi-camera panoramic images sequence and sensor/system calibration parameters. The output is the GIS-database-compatible road geometry information, which contains 3D lane line model of all the lane lines visible within cameras field of view together with line type/colour attributes. The system works in a fully automatic mode, with no operator supervision. The aim of the design is to introduce computer vision techniques to do most of the road geometry information extraction works in mobile mapping post processing, and leave as less as possible work for manual editing/correction.

There are three innovations presented in this work; first, all the visible lane lines in the georeferenced image sequences are extracted, instead of only extracting the central lane line or the nearby lane line pair. The wider cover of each MMS survey pass means less passes of the van to complete the whole survey. This makes the MMS road survey more efficient. Second, the

lane line colour/line type attributes are recognized, and therefore the output is a functional description of the road geometry. GIS database with lane lines and their attributes can better support many applications. For instance, intelligent driving assistants can tell the driver which lane to change to, not only which side to change to. Third, the output is an absolute-georeferenced model of lane lines in mapping coordinates. This means that the output is directly compatible to GIS database.

The paper is presented in 9 sections where section 2 gives the overview of the system. Sections 3 to 7 describe the design details of ARVEE. Sections 8 and 9 describe the experimental results and conclusions.

2. VISAT™ MMS OVERVIEW

VISAT™ has been developed at the University of Calgary in the early 1990s and was among the first terrestrial MMS at that time. Recently, an improved version was developed by Absolute Mapping Solutions Inc, Calgary, Canada (www.amsvisat.com), see Figure 1. The system's hardware components include a strapdown Inertial Navigation System (INS), a dual frequency GPS receiver, 6 to 12 digital colour cameras, and an integrated Distance Measurement Instrument (DMI), and the VISAT™ system controller. The camera cluster provides a 330° panoramic field of view (see Figure 2). The images are captured in sets every 2~10 meters, each of these image sets will be called a survey point. The DMI provides the van longitudinal velocities and consequently linear distances to triggers the cameras at user pre-defined constant intervals. The data-logging program, VISAT™ Log, allows for different camera configurations and different image recording distances or trigger the camera by time if necessary (both can be changed in real-time). In terms of secondary functions, the camera cluster provides redundancy, i.e. more than two images of the same object. Using the VISAT™ georeferenced images, mapping accuracies of 0.1 - 0.3 m, for all objects within the filed of view of the cameras can be achieved in urban or highway environments while operating at road speeds of up to 100 km/hr.

The user can then interface with the geo-referenced images through VISAT Station™ — a softcopy photogrammetric workstation mainly designed for manual feature extraction from georeferenced images, collected by the VISAT™ system, or any other georeferenced media. VISAT Station environment is fully integrated with ArcGIS, and permits user-friendly viewing of the imagery. Moreover, VISAT Station™ is a client/server application, enables many user terminals to access the same image data base and perform parallel processing.



Figure 1: The VISAT™ MMS Van

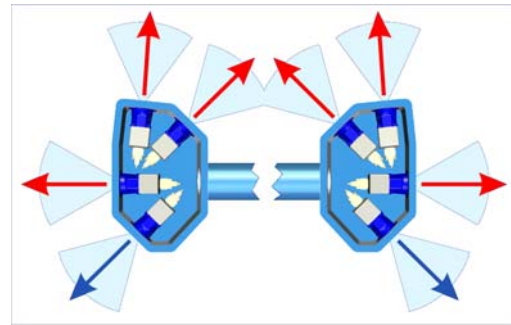


Figure 2: The VISAT™ Vision System

3. GIS FEATURE EXTRACTION FRAMEWORK

Figure 3 shows the GIS feature extraction framework for VISAT™. The input is georeferenced images acquired by the VISAT™ van. The extraction of 3D information is based on the integration of both image processing and photogrammetric analysis. The photogrammetric analysis uses available system parameters and geometrical constrains to provide a channel between 3D and 2D spaces. The image analysis extracts GIS-feature-related information in the images. Both results are used in a pattern recognition procedures, which locates the GIS features in the images and classify them into pre-specified categories. Then the GIS features are modelled in 3D to meet the requirements of GIS database.

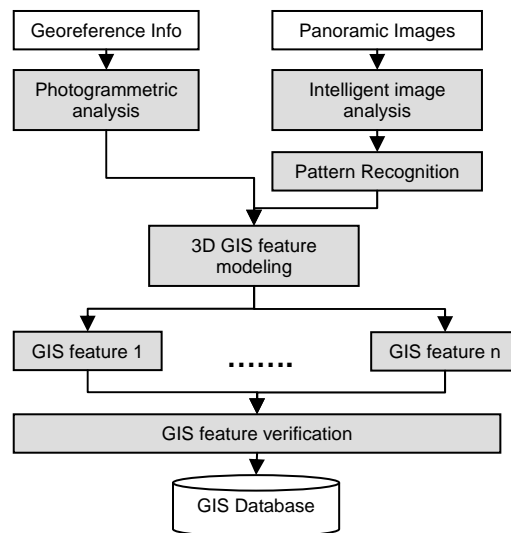


Figure 3: GIS feature extraction framework

ARVEE follows the above framework. Generally, there are two stages of processing in ARVEE. The first operates on image level by only considering images from one survey point. At this stage, linear features are extracted from each image, and projected onto a road ortho image, which is achieved by an improved inverse perspective mapping with vehicle fluctuation compensation (see section 4). Then, linear features are filtered and grouped into lane line segments (LLS). Geometric and radiometric characteristics are extracted for each LLS (see section 5). The second stage operates on high level which processes the whole MMS survey images results. All LLSs from different survey points are integrated to generate continuous lane line 3D model and their attributes. A Multiple-

Hypothesis Analysis (MHA) method is used to link the LLSs into long lane lines 3D model (see section 6). Each lane line is then classified into a lane line type, for instance “white dash line”. The classification is based on the analysis of the LLSs’ features within the lane line. A continued lane line may be of different types in difference sections, for example “white dash line” may change to “white solid line” near traffic light intersections. A decision filtering method is used to find the type-changed points (see section 7). Figure 4 shows the flowchart of ARVEE framework.

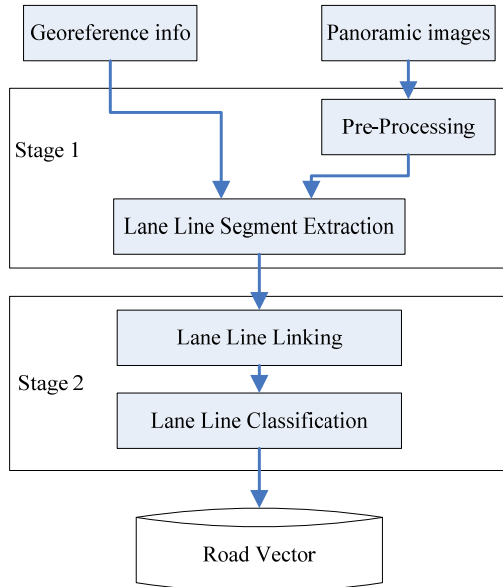


Figure 4: ARVEE Workflow

4. PITCH CORRECTED INVERSE PERSPECTIVE MAPPING (PCIPM)

The inverse perspective mapping (IPM) can be used to simplify the process of lane detection. IPM essentially re-projects the images onto a common plane (road surface plane) and provides a single image with common lane line structure. As shown in Figure 5, direction OA is the optical axis of a given camera. IG is the ideal road surface plane. Assuming the vehicle is a rigid body, the angle between OA and IG can be estimated at system calibration stage.

We denote the angle between the two vectors as $Angle(\cdot, \cdot)$. The classical inverse perspective mapping assumes that the vehicle drives on a perfect flat plane IG , and $Angle(OA, IG)$ is fixed, and the distance from camera to the road surface (denoted as H) is fixed; both $Angle(OA, IG)$ and H are known. The IPM projects all the original images from different cameras onto the IG plane, and generates the 2D ortho-image on the road surface plane, as shown in Figure 5. The generated image is no longer a perspective image but a map. In Figure 5, M is a plane parallel to IG . The ideal IPM result can be a mapping from IG to any M , through the direction that perpendicular to IG .

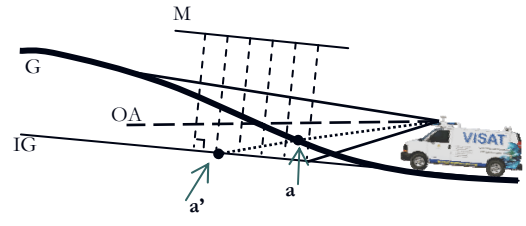


Figure 5: Classical IPM

The classical IPM is based on the flat road surface assumption. However, this assumption is not always valid in real world. There are several facts that invalidate the assumption. First, road surface is not always an ideal plane, in stead; a curved road surface is common in practice. As shown in Figure 6, given G is the true road surface, the classical IPM will project the on-road-surface point (a) to position (a'); and this will cause distortion in the resulted IPM map. Second, due to the flexibility of tires and shock absorber, vehicle is not a rigid body, the ideal IPM is violated. Therefore, given the same road surface and the same vehicle position, the angle between OA and the road surface may still be different. Third, small bumps on the road surface may cause fluctuation of vehicle, and again, this will cause OA to change.

In ARVEE, we introduce georeferencing information to overcome this problem. VISAT™ provides quite accurate measurement of the position of the body frame centre. All the cameras are fixed to the navigation body frame; and the relationship of all the sensors are accurately estimated during the system calibration.

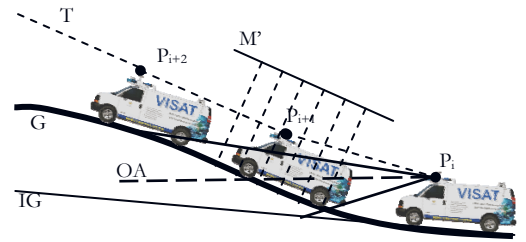


Figure 6: Pitch corrected IPM

The trajectory of the survey provides a good estimate of road surface profiles, and this model is in earth mapping frame. Given the positions of the survey points as $\{\bar{P}_i\}$, the estimation of the trajectory at position i can be expressed as

$$\bar{T}_i = F(\bar{P}_{i-m}, \dots, \bar{P}_{i-1}, \bar{P}_i, \bar{P}_{i+1}, \dots, \bar{P}_{i+n}) \quad (1)$$

where F is a trajectory interpolation function, which takes the ordered position sequence and models the trajectory. Since the road surface behind the vehicle has no influence to the IPM, so $m = 0$. The road surface are suppose to be smooth, so n can be 2, and F can, therefore, be defined as

$$F(\bar{P}_i, \bar{P}_{i+1}, \dots, \bar{P}_{i+n}) = \frac{1}{n} \sum_{j=1}^n (\bar{P}_{j+1} - \bar{P}_j) \quad (2)$$

The road surface can be described as a general cylindrical surface along the trajectory. At each point on the trajectory, the roll angle between the road surface to the body frame coordinate is 0.0. With this assumption, we correct the classical IPM according to the local trajectory at each survey point. The proceeding processing stages use this pitch-corrected road

surface (PCRS) as the a priori knowledge. As shown in Figure 6, the corrected projection is perpendicular to M' , and this eliminates most of the restoration distortions in classical IPM.

5. LANE LINE SEGMENT EXTRACTION

At each survey point, the images from all the cameras are captured at the same instant, based on distance or time, at a series of points along the route using the VISAT Log data acquisition module. The data acquisition module, VISAT Log, can be configured on the fly to trigger the cameras for any desired distance. In urban surveys, this distance is typically 3 to 5 meters intervals between image sets, which will ensure complete panoramic coverage. On highways, 5 to 10 meters intervals are typically used. At each survey point, the cameras cover a wide angle of the surrounding area. The aim of LLS extraction is to extract the lane lines within the covered area from each image set captured at the same survey point. ARVEE is adaptive to different camera configurations, which greatly increase the flexibility. This convention is due to the effective LLS extraction algorithm.

For each camera, the image is applied with a linear feature extraction algorithm (Cheng Wang, 2002). All the lane line associated linear features are filtered by the following constrains:

- (1) Shape constrain: the lane lines is supposed to be a solid or dashed line with a certain width;
- (2) Colour constrain: the lane lines usually are of white or yellow colour, and
- (3) Geometry constrain: the road is a flat surface and the lane line is with a small curvature.

The filtered out linear features from different cameras are added into the lane-line-associated linear feature set (**LALS**). All the elements in **LALS** are combined to establish the 3D model of the **LALS** in the mapping frame. In this stage, more constrains are introduced to determine is the location of the LLSs and their central lines. These constrains are mainly from the observational correspondence across cameras. The major constrains include: (1) Space distribution correspondence: the observations to the same LLS from different cameras should be close to each other in PCRS. (2) Colour distribution correspondence: the LLS should have similar colour distribution in difference observations, and (3) Heading direction agreement: all the LLSs should agree to the heading direction of the road. At this stage, attributes that describe the characteristics of each LLS are also extracted. These attributes will later be used to classify the lane line type. For each LLS, as shown in Figure 7, the local image is separated into three parts: the lane line covered region **C**, the left neighbour region **L** and right neighbour region **R**.

Motivated by common features used by human, ARVEE utilizes the following features to describe a LLS: relative position and orientation to the body frame centre; dashness (the dash-shape of the LLS); colour distribution of region **C**, **L**, **R**; the relationship between the three colour distributions; and texture features.

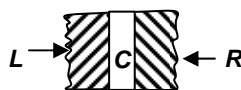


Figure 7: Local image segmentation for feature extraction

6. MULTI-HYPERTHESIS LINKING

Given the LLSs extracted from each survey point, the aim of lane line linking is to join the LLSs through the whole survey image sets to form a continuous 3D model of the lane lines. Each lane line could include several to hundreds of LLSs. Multi-hypothesis Analysis (MHA) has proved to be successful in many applications, such as multi-target tracking (Gong, 2005). ARVEE utilizes a revised MHA algorithm to perform the lane line linking. The MHA has three steps: hypothesis generation; likelihood computation; and hypotheses management.

All the LLSs are kept in a graph structure as shown in Figure 8. Each node represents a LLS. For instance, node $L_{i,j}$ is the j th LLSs in i th survey image set. The lane line linking develops the edges connecting the nodes. At each survey point, the hypotheses are the possible connecting configurations between the ends of current maintained node to the nodes in the future image sets.

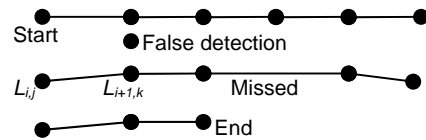


Figure 8: Graph structure for multi-hypotheses analysis

The hypothesis generation step first calculates the possibility of the connections between the maintained graph nodes and the nodes from the current image set. The maintained nodes include the ending nodes of all the links in maintained hypotheses. They are not necessarily from the previous image set since LLS extraction may have misdetections. The connection probability is computed as:

$$P_{con} = w_p p_p + w_d p_d + w_f p_f \quad (3)$$

where p_p is the position closeness possibility between the new node to the maintained note, p_d is the direction similarity possibility, p_f is the feature similarity; and w_p w_d w_f are the weights of this probabilities. In hypotheses generation step, all the possible connection configurations are added to hypothesis list. Then, hypotheses with low connection possibility are pruned out of the list.

Given the hypotheses (the connections configurations) obtained from the previous processing, the likelihood calculation step calculates the likelihood of each new hypothesis. This step introduces the information of all the maintained hypotheses, to bring in an overall view of the LLS graph. The likelihood is calculated as:

$$likelihood_i = \begin{cases} likelihood_{i-1} + \frac{\sum_j^n w_{con} P_{conj} + w_{trj} P_{trjj} + w_{feaj} P_{feaj}}{n} & \text{Condition*} \\ 0 & \text{otherwise} \end{cases} \quad (4)$$

where i is the current image set number, n represent the number of objects in the current hypothesis. P_{conj} is the connection probability of the j th connection; P_{trjj} is the smoothness probability of the new connection to the former link; P_{feaj} is the feature similarity possibility. W_{con} , W_{trj} , and W_{feaj} are the weights to these possibilities. **Condition*** represents a set of constrains that make a hypothesis possible. The constrains include: no multiple connection; and no crossing connection. These constrains express the nature of a possible lane line.

With the increase of the survey image sets, the size of the hypothesis set might quickly explodes. Hypothesis management step is designed to keep a practical-sized hypothesis set and keep the diversity of that hypothesis set as much as possible. Several rules are introduced: first, only limited amount of hypotheses are maintained; second, the hypotheses that are not changed for several image sets will be combined into other hypotheses, or deleted; third, only limited hypotheses are allowed to be added at each image set.

The MHA processing goes through all the image sets. At the end, H^* —the hypothesis with highest likelihood— will be viewed as the best connection configuration of all the LLS notes. Each links in H^* is a lane line.

7. LANE LINE CLASSIFICATION

The classification of LLS attributes is affected by many facts: occlusion; worn-out painting of lane lines; variation of the side pavements or grass; variance of road surface materials; and the unreliability of the feature extraction algorithms. So, instead of classify the LLS, we calculate the feature of a lane line base on all the LLSs included in that lane line; and classify the type of the lane line as a whole.

Lane line usually extends for hundreds of meters or even kilometers. According to the traffic design, the type of lane line may change during the extension. For example, a dashed white lane line may change into a solid near road crossings, to keep the vehicles from lane change. However, the above mentioned lane line detection and linking procedures are not able to separate the lane line type changes. In order to solve this problem, type-changed point detection is introduced in our system.

Denote a lane line as LA , LA includes a set of LLS, $LA = \{l_i | i=0,n\}$. Denote judge function E_i as :

$$E_i = \begin{cases} 0 & \text{when } F(l_{i-d}, \dots, l_i) = F(l_{i-d}, \dots, l_i) \\ 1 & \text{when } F(l_{i-d}, \dots, l_i) \neq F(l_{i-d}, \dots, l_i) \end{cases} \quad (5)$$

where d is the buffer size. $F(l_k, \dots, l_p)$ is the classification function that decide the lane line type based on the characteristics of LLSs $\{l_k, \dots, l_p\}$. In practice, we use a KNN classifier as $F()$. If the preceding lane line segments l_{i-d}, \dots, l_i and the successive lane line segments l_{i-d}, \dots, l_i are not with the same type, then E_i is 1, and LLS l_i is viewed as a point where the lane line type changed. Figure 9 illustrate the finding of type-changed point.

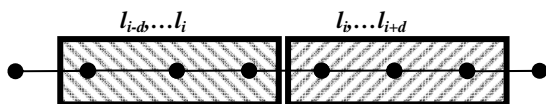


Figure 9: detection of type-changed point

Once a type changed point is detected, the lane line will be broken at that point. The separated two parts of the lane line are to be classified independently.

8. EXPERIMENTS

ARVEE has been tested over massive real mobile mapping survey data from VISAT™, including data from urban and rural

areas. Test results show that ARVEE is robust and ready to serve the real world applications. Video of the results can be found at http://mms.geomatics.ucalgary.ca/Team/Current/Collaborators/cheng/AVREE_demo/ARVEE_demo.htm

Figure 10 shows a road geometry extraction result of ARVEE. The extracted lane lines are superimposed on the original images (only two of the four cameras are shown in the figure). There are four lane lines within this site, all correctly extracted and classified. The two lines in the middle of the road are dashed white lane line (marked as dashed white line), the one in the left is a yellow solid lane line (marked as solid yellow line), and the one on the right side is a solid white line (marked as solid white line). Figure 11 is the bird eye view of the extracted road geometry. At this point, it should be stressed that, although there are other vehicles occlude the sight view to the right side lane line, it is still successfully extracted. This shows the robustness of the ARVEE against partly occlusion.

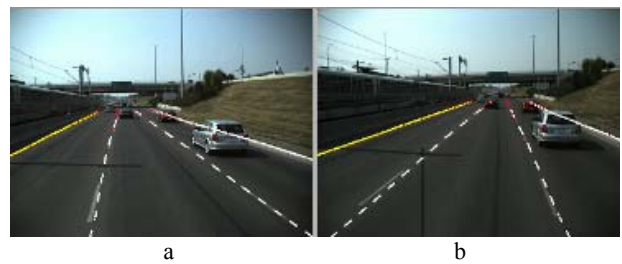


Figure 10: ARVEE result in partly occlusion

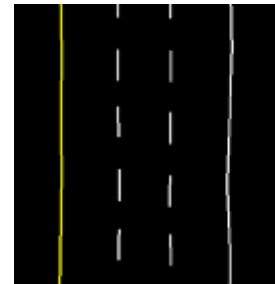


Figure 11: Bird eye view of result in Figure 10

Figure 12 shows ARVEE result at a shadowed road. Despite of the tree shadows, all visible lane lines are correctly detected, linked and classified. This shows the robustness of the ARVEE against shadows.



Figure 12: Road geometry result in shadows

Figure 13 shows the detected road geometry overlapped on the digital map. The extracted road geometry fits the map perfectly, but with much more details and much higher accuracy. The result can greatly improve the current GIS database.

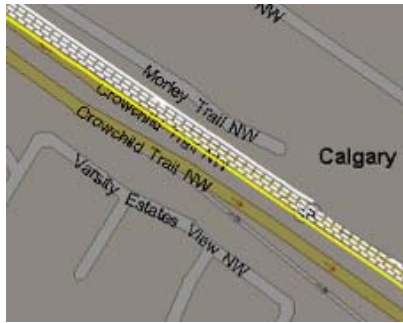


Figure 13: ARVEE result overlapped on map

In order to evaluate the misdetection rate and false detection rate of ARVEE, over 25 kilometres (more than 100,000 meters lane lines) survey data are first automatically processed by ARVEE, and then corrected manually. The manually corrected result (MCR) is viewed as a reference, and compared with the automatic result (AR). All the lane lines appear in MCR but not in AR are count as misdetection (MD), and all the lane lines appear in AR but not in MCR are viewed as false detection. The misdetection and false detection rate is calculate based on the length of the lane lines. The statistics of the test are shown in Table 1.

	Length (meter)	Percentage
Total Lane Line	102,732	100%
False detection	9,889	9.62%
Miss-detection	2,510	2.4%

Table 1: Performance statistics of ARVEE

The major causes of the misdetection are worn-out lane lines, and heavy occlusion. The major causes of false detection are lane-line-similar structures near the road, such as the edge of side walks, or the line shapes in the nearby vehicles. Figure 14 and Figure 15 show examples of misdetection and false detection. In Figure 14, there is a worn-out dashed white lane line in the right side of the road, and is misdetections.



Figure 14: Example of miss detection to worn-out lane line



Figure 15: Example of false detection in heavy occlusion

9. CONCLUSION

MMS are efficient and cost effective tools for building and updating GIS databases. However, manual measurements of GIS features in MMS are still manpower demanding procedure. We have initiated a wide scope project for automated GIS features extraction, to decrease and possibly eliminate the most of the human work in the post-processing. In this paper, we present ARVEE, a robust automatic functional road geometry extraction system for MMS. There are three innovations in ARVEE. First, instead of only extracting the central lane line or the nearby lane line pair, our system extracts all the visible lane lines in the georeferenced image sequences. Second, the lane line attributes are recognized, so the output is a functional description of the road geometry. Third, the output is the high accurate absolute-georeferenced models which are compatible to the GIS database. Test over massive real mobile mapping demonstrate that ARVEE are ready for the real world applications.

10. REFERENCE

- El-Sheimy, N. and K.P., S., 1999. Navigating Urban Areas by VISAT - A Mobile Mapping System Integrating GPS/INS/Digital Cameras for GIS Applications. *Navigation, Journal of the USA Institute of Navigation Journal*, 45(No. 4), pp. 275-286.
- Ishikawa, S., Kuwamoto, H., et al., 1988. Visual navigation of an autonomous vehicle using white line recognition. *IEEE Transactions on Pattern Analysis and Machine Intelligence*, 10(5), pp. 743-749.
- Kenue, S. K., 1991, LANELOK. An algorithm for extending the lane sensing operating range to 100 feet. *Proceedings of SPIE - The International Society for Optical Engineering*, Boston, MA, USA, 1388, pp. 222-233.
- Jochem, T. M., Pomerleau, D. A., et al., 1993, "MANIAC": A Next Generation Neurally Based Autonomous Road Follower. *Image Understanding Workshop*, pp. 473-479.
- Chen, K. H. and Tsai, W. H., 1997. Vision-based autonomous land vehicle guidance in outdoor road environments using combined line and road following techniques. *Journal of Robotic Systems*, 14(10), pp. 711-728.
- Beauvais, M. and Lakshmanan, S., 2000. CLARK: A heterogeneous sensor fusion method for finding lanes and obstacles. *Image and Vision Computing*, 18(5), pp. 397-413.
- Paetzold, F. and Franke, U., 2000. Road recognition in urban environment. *Image and Vision Computing*, 18(5), pp. 377.
- Yim, Y. U. and Oh, S.-Y., 2003. Three-feature based automatic lane detection algorithm (TFALDA) for autonomous driving. *IEEE Transactions on Intelligent Transportation Systems*, 4(4), pp. 219-225.
- Li, Q., Zheng, N., et al., 2004. Springrobot: A prototype autonomous vehicle and its algorithms for lane detection. *IEEE Transactions on Intelligent Transportation Systems*, 5(4), pp. 300-308.

McCall, J. C. and Trivedi, M. M., 2004, An integrated, robust approach to lane marking detection and lane tracking. IEEE Intelligent Vehicles Symposium, Proceedings, Parma, Italy, pp. 533-537.

Tai, J.-C., Tseng, S.-T., et al., 2004. Real-time image tracking for automatic traffic monitoring and enforcement applications. *Image and Vision Computing*, 22(6), pp. 485.

Wang, Y., Teoh, E. K., et al., 2004. Lane detection and tracking using B-Snake. *Image and Vision Computing*, 22(4), pp. 269-280.

Hassouna, M. S. and Farag, A. A., 2005, Robust centerline extraction framework using level sets. Proceedings. 2005 IEEE Computer Society Conference on Computer Vision and Pattern Recognition, San Diego, CA, USA, vol. 1, pp. 458-465.

Jung, C. R. and Kelber, C. R., 2005. Lane following and lane departure using a linear-parabolic model. *Image and Vision Computing*, 23(13), pp. 1192.

Lee, J. W. and Yi, U. K., 2005. A lane-departure identification based on LBPE, Hough transform, and linear regression. *Computer Vision and Image Understanding*, 99(3), pp. 359.

Choi, S. Y. and Lee, J. M., 2006. Applications of moving windows technique to autonomous vehicle navigation. *Image and Vision Computing*, 24(2), pp. 120-130.

Kastrinaki, V., Zervakis, M., et al., 2003. A survey of video processing techniques for traffic applications. *Image and Vision Computing*, 21(4), pp. 359.

Goldbeck, J., Huertgen, B., et al., 2000. Lane following combining vision and DGPS. *Image and Vision Computing*, 18(5), pp. 425-433.

Wang, J., Schroedl, S., et al., 2005. Lane keeping based on location technology. *IEEE Transactions on Intelligent Transportation Systems*, 6(3), pp. 351-356.

Tao, C. V., Chapman, M. A., et al., 2001. Automated processing of mobile mapping image sequences. *ISPRS Journal of Photogrammetry and Remote Sensing*, 55(5-6), pp. 330-346.

Roncella, R. and Forlani, G., 2006, Automatic lane parameters extraction in mobile mapping sequences. *ISPRS Image Engineering and Vision Metrology 2006*.

Wang, C., Wen, G.-J., et al., 2002. Line extraction for broadband image signals. *Jisuanji Xuebao/Chinese Journal of Computers*, 25(7), pp. 753-758.

Gong, Y., 2005. Integrated object detection and tracking by multiple hypothesis analysis. *NEC Journal of advanced technology*, Vol. 2(No. 1), pp. 13-18.

